International Symposium
On Turbulence and Shear Flow
Phenomena (TSFP-8)
August 28 - 30, 2013 Poitiers, France

LOCAL FORCING OF LAMINAR SEPARATION BUBBLES

E. Kaiser, A. Spohn, L. Cordier, B. R. Noack
Department Fluides, Thermique, Combustion, CEAT
Institut PPRIME, CNRS-Université de Poitiers-ENSMA, UPR 3346
43 rue de l'Aérodrome, F-86036 Poitiers CEDEX, France
eurika.kaiser@univ-poitiers.fr

ABSTRACT

Local forcing of laminar separation bubbles has been studied inside a low-speed water tunnel. Flow separation is induced by a canonical pressure distribution along a smooth ramp. Flow instabilities are excited by oscillating a thin horizontal wire which is placed inside the boundary layer upstream of separation. The diameter of the wire measures only $1/100$ of the boundary layer thickness and its Reynolds number remains $O(1)$. The spatial and temporal evolution of the separated shear layer is analysed with high-resolution visualisations using the electrolytic precipitation technique. Time-resolved flow visualisations obtained with the hydrogen bubble technique and PIV measurements are used to analyse the reattachment zone of the laminar separation bubble.

Using all these techniques the laminar separation bubbles are found to be highly sensitive to local forcing upstream of flow separations. Periodic oscillations of the wire in the wall-normal direction produce significant changes in the spatial and temporal evolution of the separation bubble. In the upstream part of the separation bubble the beginning growth of the most amplified mode can be precipitated close to the separation line. At the same time the bubble length can be reduced up to 50% by periodic forcing with the natural shedding frequency. All these results confirm previous numerical studies of Rist & Augustin (2006) which predict the possibility to control laminar separation bubbles by local forcing upstream of flow separation. In the near future, we shall apply this highly efficient and flexible technique to perform closed-loop control of laminar separation bubbles in combination with optical sensors.

INTRODUCTION

In recent years laminar separation bubbles (LSB) have received increasing attention due to their impact on performance losses in numerous aerodynamic applications. Examples range from wind turbines, unmanned aerial vehicles (UAVs) to internal flows in turbomachinery. LSB occur when laminar flow is forced to detach from the wall, giving rise to a newly-formed separated shear layer, which penetrates into the flow domain. The development of flow instabilities along this shear layer often leads to laminar-turbulent transition and reattachment. To reduce the drawbacks on lift and drag forces caused by LSB, there have been many attempts to diminish the extensions of LSB by exciting the Kelvin-Helmholtz instability (Dovgal *et al.*, 1994). According to Huerre & Rossi (1998) the separated shear layer acts, like in the case of a mixing layer, as a noise amplifier. Previous experimental studies employed loudspeakers (Gaster, 1967), pulsating jets (Kiya *et al.*, 1993; Sigurdson, 1995) or plasma actuators (Huang *et al.*, 2003) to force the flow. In numerical studies local periodic forcing has been simulated by sources with time-dependent strength (Chung *et al.*, 1997). Although all these techniques had a significant impact on the flow structure, the complex interaction of these actuators with the flow field and the at least in the downstream part of the LSB highly nonlinear flow behaviour, this did not yet allow to understand the control mechanism. In particular, it has been recognized in recent years that for efficient and flexible control of flow separation it is necessary to design closed-loop control with a precisely defined actuator signal in combination with feedback information. Numerical studies of Rist & Augustin (2006) and Diwan & Ramesh (2009) showed that two-dimensional and three-dimensional perturbations, inside the boundary layer upstream of separation, can be amplified, making them a good candidate to excite the separated shear layer. Consequently, they suggested to install wall mounted oscillating disturbance strips upstream of flow separation to suppress the formation of bubbles by periodic oscillations. To obtain lowest drag penalties on airfoils they further proposed to activate these actuators only when skin friction sensors detect the existence of LSB. High frequencies of $O(10^3)\,Hz$ and small dimensions of $O(10^{-3})\,m$ hindered so far experimental tests of such a control system.

The goal of this study is to elucidate the potential of using two-dimensional perturbations upstream of separation for open- and closed-loop control of flow separation. To this end, we took advantage of a low-speed water tunnel to increase the characteristic time and length scales, thus facilitating the experimental investigation. A smooth ramp geometry was chosen to induce the natural formation of LSB under controlled experimental conditions. In order to obtain a highly flexible and simple flow excitation, a thin movable wire was fixed parallel to wall inside the boundary layer upstream of separation. Complementary time-resolved flow visualisations and PIV measurements are used to analyse the impact of forced oscillations on vortex shedding and bubble length. The results show, despite the small diameter of the wire of about $1/100$ of the boundary layer thickness and despite its small Reynolds number of $O(1)$, a significant impact on the spatial and temporal evolution of the separation bubbles. With periodic forcing the bubble length is reduced up to 50%. All these observations demonstrate that LSB can be forced by the wire actuator efficiently. Based on this actuator we plan in the near future to design closed-loop control for LSB in combination with optical sensing

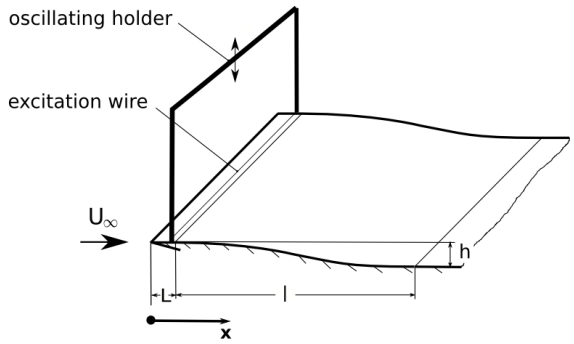

Figure 1: Schematic of the canonical flow configuration and the arrangement of the actuator wire.

of the flow state. Thereby the observed relaxation times of $O(1)$ seconds suggest that even low-cost hardware can be sufficient to calculate the plant output in time.

EXPERIMENTAL SET-UP

The flow has been studied in a low-speed water tunnel to facilitate time-resolved flow visualisations and PIV measurements. The test section with a free surface is $2.1\,m$ long, $0.5\,m$ wide and $0.34\,m$ high. Fig. 1 shows a schematic of the smooth ramp model and the arrangement of the actuator wire. The leading edge of the model which is composed of a sharp wedge with an angle of 15°, divides the upstream flow into the flow along the ramp and the flow beneath the model.

Beginning from the leading edge a laminar zero pressure gradient boundary layer develops along the flat plate of length $L = 100\,mm$. Above the smooth ramp of height $h = 60\,mm$ and length $l = 600\,mm$ this boundary layer separates under the influence of an adverse pressure gradient which is fixed by the shape of the ramp. The ramp contour follows a polynomial shape of order 7 for which Sommer (1965) numerically determined the position of the LSB. The flow model is $498\,mm$ wide and covers the whole width of the test section with the exception of two $1\,mm$ wide gaps between the tunnel walls and the ramp. Downstream of the ramp a horizontal plate prolongates the separation between the upper and lower flow to reduce the impact of temporal changes in the flow structure during forcing. The stagnation point on the leading edge was controlled by adjustable pressure losses at the outlet of the upper flow. The Reynolds number $Re = UL/\nu$, based on free-stream velocity U, and the kinematic viscosity ν of water, varied between $O(10^3)$ and $O(10^4)$.

In this study, locally-controlled forcing was enabled by employing a stainless steel wire of $0.13 \pm 0.01\,mm$ in diameter, which was supported by an oscillating holder. The wire crossed the whole span of the model $90 \pm 2.5\,mm$ downstream of the leading edge. To impose to the wire a vertical sinusoidal motion we used either an electromagnetic vibrator (Brüel & Kjoer, Power amplifier type 2706) in combination with a frequency generator (Stanford Research Systems, model DS 345) or a line servo (RS-2 modelcraft) which was piloted by an Arduino-Due microprocessor. The frequency ranged between 0.1 and $3\,Hz$. The oscillation amplitude was smaller than $3 \pm 1\,mm$. In all experiments the mean position was fixed at $3.5 \pm 0.5\,mm$.

To analyse the flow we used complementary techniques. The global velocity field was measured with a commercial PIV system (LAVision) using JAI ($1600 \times 1200\,pix$) Cameras and a YAG laser. Typical spatial resolutions were $0.239\,mm$ per pixel for the global flow field and $0.071\,mm$ per pixel to measure the velocity profile inside the boundary layer. Flow visualisations obtained with the electrolytic precipitation technique (Taneda & Tomonari, 1974) were used to analyse the spatial and temporal growth of the forced perturbations along the separated shear layer. A solder wire, which is $0.08 \pm 0.01\,mm$ thick and $4 \pm 0.5\,mm$ large, was fixed flash to the wall of the ramp $300 \pm 5\,mm$ downstream of the leading edge. White tracer particles, which are transported with the flow, are released by applying a positive voltage in the range of 2 to 10 Volts between this solder wire and a reference electrode placed at the end of the test section. An Argon laser with $3W$ had been used to illuminate these tracers in the middle plan of the test section by expanding the light beam to a sheet of light. In this way, the actual position of the separation line and of the separated shear layer became visible. To study the reattachment zone the hydrogen bubble technique (Schraub *et al.*, 1965) turned out to be more useful. For that purpose, a $0.050 \pm 0.005\,mm$ thick stainless steel wire was deformed into a zigzag pattern and fixed in the middle of the ramp at about $300 \pm 5\,mm$ downstream of the leading edge. When applying a negative potential, between 30 and 90 Volts, hydrogen bubbles were produced at the wire and fed further downstream. A computer controlled function generator allowed to trigger the release of bubbles to obtain periodic timelines. These timelines mark vortical structures and patches of the reattaching flow.

RESULTS

Figure 2 illustrates the effect of periodic forcing on the laminar separation bubble. Both visualisations were obtained with the electrolytic precipitation. Once released on the wall by the solder wire, the white tracer is pushed in the direction of the separation line by the wall shear stress. Near the separation line diffusion becomes predominant and the tracer is diffused away from the wall towards the interior of the flow domain. Finally, the tracer is further entrained along the separating shear layer, where the tracer remains visible as a sharp line, since inside the flow domain the Schmidt number is high ($Sc > 10000$). In Fig. 2 (a), without forcing, the white particles advance at first along the upstream part of the bubble nearly horizontally. Then, naturally growing instabilities deform the separated shear layer towards the downstream end of the bubble, and finally, the roll-up of the tracer line marks the formation of Kelvin-Helmholtz vortices. These highly two-dimensional vortices become rapidly unstable with respect to secondary instabilities as indicated by the blurring of the tracer further downstream. In contrast periodic forcing, shown in Fig. 2 (b), leads already in the upstream part of the bubble to rapidly increasing vertical deformations of the shear layer. At the same time the separated shear layer gets closer to the wall and the position of flow separation moves in the downstream direction from $x_{s,n} = 268 \pm 2\,mm$ to $x_{s,f} = 287 \pm 2\,mm$. The curled tracer distributions at the end of the bubble points to a reinforced periodic emission of highly two-dimensional vortical structures. Clearly periodic actuation has a major impact on the flow by reducing the height and length of the laminar separation bubbles.

The hydrogen bubble technique gives indications on

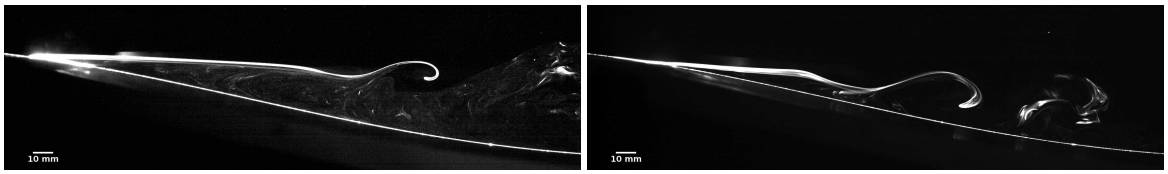

(a) (b)

Figure 2: Visualisation of the separated shear layer at $Re = 7700$ with the electrolytic precipitation technique: (a) without excitation, and (b) with periodic forcing at $f_e = 0.56\,Hz$ and amplitude $3\,mm$. Clearly vortex shedding sets in earlier and reduces the length of the separation bubble.

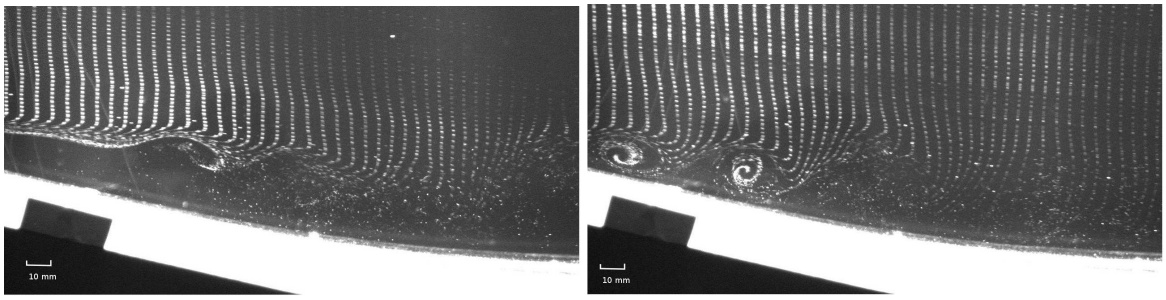

(a) (b)

Figure 3: Visualisation of the reattachment region at $Re = 7700$ with the hydrogen bubble technique. The bubble wire is located upstream of flow separation (a) without excitation, and (b) with periodic forcing at $f_e = 0.64\,Hz$ and amplitude $3\,mm$. In the forced case the hydrogen bubbles reveal that the vortices carry periodically fluid from inside the flow domain towards the wall.

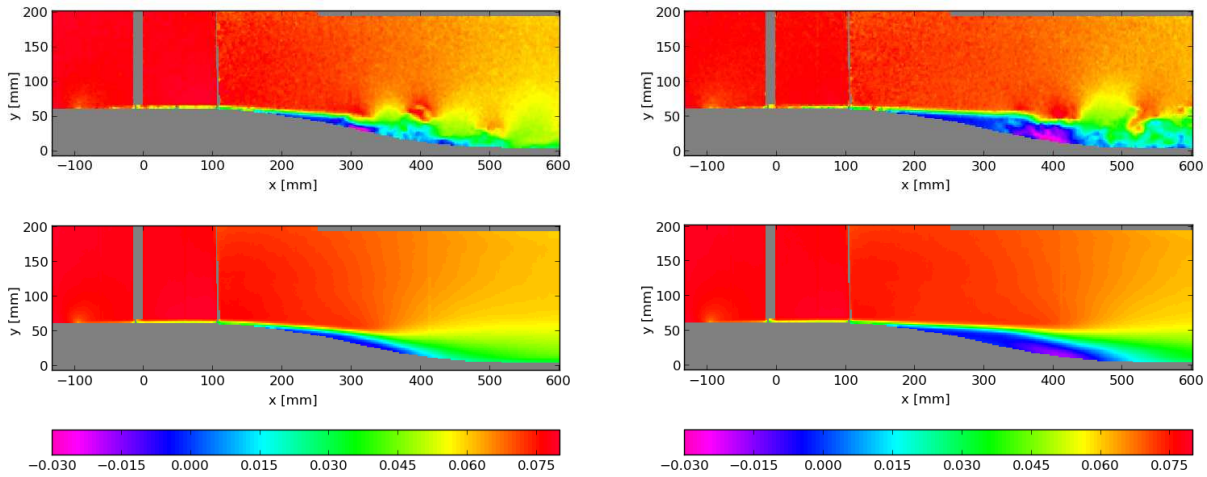

(a) (b)

Figure 4: Comparison of the instantaneous (above) and mean velocity fields (below) at $Re = 7700$ for two different excitation frequencies (a) $f_e = 0.31\,f_n$, and (b) $f_e = 2.46\,f_n$. The excitation has a clear impact on the spatial and temporal evolution of the shear layer and the surrounding mean velocity field.

the flow behaviour during the reattachment process at the end of the separation bubbles. Figure 3 shows snapshots of the hydrogen bubble distribution in the reattachment zone with and without forcing. The hydrogen bubbles are released upstream of separation. Therefore, without forcing no tracers are visible inside the upstream part of the separation zone in Fig. 3 (a). Further downstream Kelvin-Helmholtz vortices carry the bubbles towards the wall without reaching it. The entrainment of fluid from the main flow towards the wall remains limited to the region where white tracer particles are visible. In Fig. 3 (b) with forcing, the more rapid formation of Kelvin-Helmholtz vortices leads to patches of reattaching flow as indicated by periodic presence of hydrogen bubbles near the wall. The related increased entrainment of fluid from the main flow leads to shorter separation bubbles.

Quantitative information on the effect of local forcing were obtained from PIV measurements. By using an increased spatial resolution of $0.071\,mm$ per pixel the momentum thickness Θ at separation was found to be about $1.6\,mm$ thick. Following Ho & Huerre (1984) this leads to a natural shedding frequency $f_n = 0.57\,Hz$ in good agree-

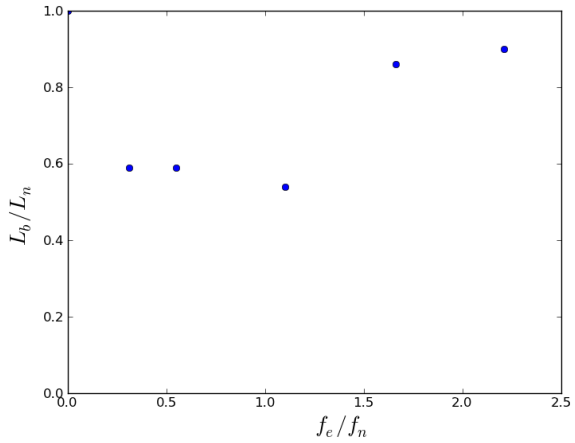

Figure 5: Nondimensional bubble length versus nondimenisonal forcing frequencies. The smallest bubble length is obtained in the vicinity of the natural shedding frequency af $f_e = f_n$.

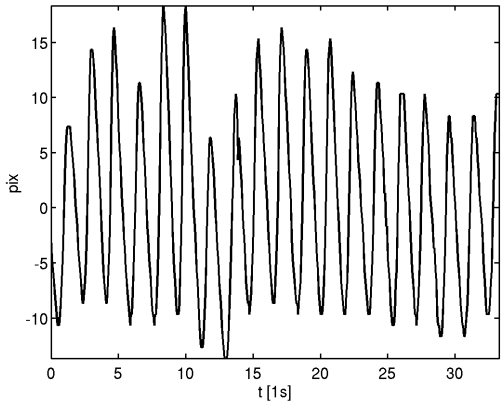

Figure 6: Oscillations of the forced separated shear layer at $x/x_{s,f} = 1.25$ for $Re = 7700$.

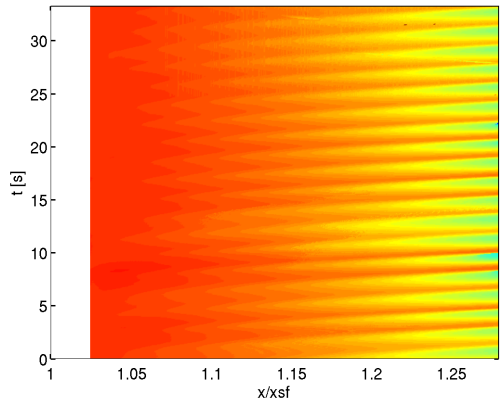

Figure 7: Spatiotemporal diagram of the tracer height for the forced flow at $Re = 7700$.

ment with the shedding frequency evaluated from image sequences. Figure 4 compares the instantaneous and mean velocity fields for two different excitation frequencies. For the excitation frequency $f_e = 0.31\ f_n$ the mean length of the bubble becomes about 40% shorter and at the same time the pressure recovery in the mean flow increases as indicated by the rapid decrease of the mean velocities in the downstream direction. In contrast, for $f_e = 2.46\ f_n$ the separated shear layer, visible in the instantaneous velocity field, is more stable. The bubble length decreases only slightly leading to less pressure recovery. The bubble length was determined more precisely by calculating the reverse flow time fraction from PIV measurements over 55.6 periods of the natural shedding frequency. Without excitation the bubble length L_n was found to be $325\,mm$ long. The evolution of the nondimensional bubble length L_b/L_n as a function of the nondimensional excitation frequency f_e/f_n is shown in Fig. 5. The most significant reduction of L_b/Ln of about 50% is achieved in the vicinity of $f_e = f_n$.

In order to analyse the flow mechanisms generated by the local periodic forcing in more detail we took advantage of the sharp line which is characteristic for flow visualisations obtained with the electrolytic precipitation technique. Similar to the PLIF technique used by Julien *et al.* (2003) in the case of a wake flow, the deformations of the sharp line are the consequence of the growth of the instabilities along the separated shear layer. The temporal evolution of the position of the sharp line at each x position along the separated shear layer was determined with routines implemented in Matlab using the Signal Processing Toolbox. These measurements were extracted from a sequence of 500 images which was taken at 15 frames per second. Examplarly, Fig. 6 illustrates the highly periodic character of such a signal in the actuated case at $x/x_{s,f} = 1.25$.

The phase velocity of the most amplified mode is measured employing a two-dimensional spatiotemporal diagram of the tracer height for the forced separated shear layer as presented in Fig. 7. As indicated by the front of the progressing wave crest the phase velocity achieves nearly $4.4\,cm/s$.

Individual spatial growth rates of different modes are determined by aligning the most significant amplitudes of the Fourier decomposition of each of these local signals. However, this technique is only appropriate up to the position where the roll-up by vortices leads to ambiguous dislocations of the tracer. Figure 8 compares the spatial evolution of the most amplified modes for unforced and periodically forced flow at $Re = 7700$. All distances in the x direction are measured with respect to the position of the separation line of the respective shear layers. In the case of natural flow, shown in Fig. 8 (a), only the most unstable mode begins to grow significantly towards the end of the bubble. The same mode is entrained much closer to the separation line in the case of periodic forcing at f_n as displayed in Fig. 8 (b). The slope of its increasing amplitude indicates a spatial growth rate of $0.049\,mm^{-1}$. Subharmonic entrainment is also visible.

All of these results confirm nicely the validity of the linear instability theory in the upstream part of the separation bubble. As mentioned above this region is followed by the roll-up of vortices which give the flow a nonlinear dynamics which has to be analysed in more detail.

CONCLUSIONS

The experiments presented in this study demonstrate that highly two-dimensional small perturbations upstream of flow separation are sufficient to reduce the length of lam-

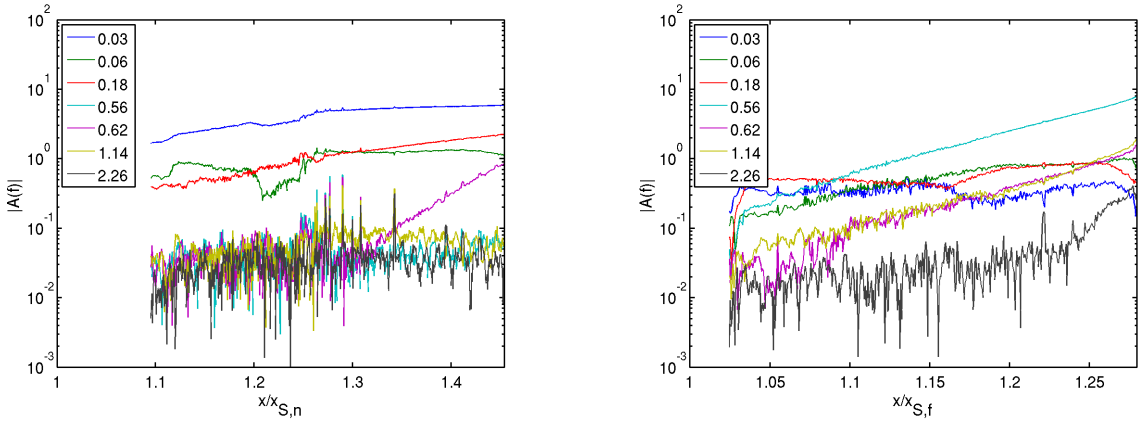

(a) (b)

Figure 8: Comparison of the spatial evolution of the most amplified modes of (a) natural flow, and (b) flow forced with $f_e = f_n$ at $Re = 7700$.

inar separation bubbles up to 50%. For that purpose, the newly developed oscillating wire arrangement turned out to be a highly efficient and flexible actuator. All these results confirm previous numerical studies of Rist & Augustin (2006) which predict the possibility to control laminar separation bubbles by local forcing upstream of flow separation. Although the upstream part of the separation bubble showed a linear response to excitation, further investigations by pulsed oscillations are needed to clarify the contributions of vortex formation and shedding to the global flow response. By adjusting the frequency, phase and amplitude of the excitation we plan to perform closed-loop phasor control based on a reduced-order model of the flow, following Pastoor *et al.* (2006) and incorporating innovations of Noack *et al.* (2011).

ACKNOWLEDGMENTS

This work is supported by the French Agence Nationale de la Recherche Projet ANR-11-BS09-018 SepaCoDe. The first author acknowledges for funding by the NSF PIRE grant OISE-0968313. All authors acknowledge the funding and excellent working conditions of the Chaire of Excellence “Closed-loop control of turbulent shear flows using reduced-order models” (TUCOROM) supported by the French Agence Nationale de la Recherche (ANR) and hosted by Institute PPRIME. We appreciate valuable stimulating discussions with the SepaCoDe team, in particular Azeddine Kourta and Michel Stanislas, with the TUCOROM team, in particular Markus Abel, Jean-Paul Bonnet, Jacques Borée, Joël Delville, Robert Niven and Michael Schlegel. Special thanks are due to Nadia Maamar for a wonderful job in hosting the TUCOROM visitors.

REFERENCES

Chung, Y.M., Kim, Y. & Sung, H.J. 1997 Large-scale structure of leading-edge separation bubble with local forcing. *Fluid Dyn. Research* **19**, 363–378.

Diwan, S. S. & Ramesh, O. N. 2009 On the origin of the inflectional instability of a laminar separation bubble. *J. Fluid Mech.* **629**, 263–298.

Dovgal, A. V., Kozlov, V. V. & Michalke, M. M. 1994 Laminar boundary layer separation: instability and associated phenomena. *Prog. Aerosp. Sci.* **30**, 6194.

Gaster, M. 1967 The structure and behaviour of separation bubbles. *ARC R & M* **3595**.

Ho, C. M. & Huerre, P. 1984 Perturbated free shear layers. *Ann. Rev. Fluid Mech.* **16**, 365–424.

Huang, J., Corke, T. C. & Thomas, F. O. 2003 Plasma actuators for separation control of low pressure turbine blades. *AIAA Paper 2003-1027* pp. 365–424.

Huerre, P. & Rossi, M. 1998 Hydrodynamic instabilities in open flows. *In Hydrodynamics and Nonlinear Instabilities* pp. 81–294.

Julien, S., Lasheras, J. & Chomaz, J.-M. 2003 Three-dimensional instability and vorticity patterns in the wake of a flat plate. *J. Fluid Mech.* **479**, 155–189.

Kiya, M., Moehizuki, O., Ido Y. & Kosaku, H. 1993 Structure of turbulent leading-edge separation bubble of a blunt circular cylinder and its response to sinusoidal disturbances. *J. Wind Eng. Ind. Aerod.* **49**, 227–236.

Noack, B. R., Morzynski, M. & Tadmor, G. (eds.) 2011 *Reduced-Order Modelling for Flow Control*. Springer Verlag Vienna.

Pastoor, M., Noack, B. R., King, R. & Tadmor, G. 2006 Spatiotemporal waveform observers and feedback in shear layer control. *AIAA Paper 2006-1402, 44th AIAA Aerospace Sciences Meeting and Exhibit Reno,NV,USA* .

Rist, U. & Augustin, K. 2006 Control of laminar separation bubbles using instability waves. *AIAA Journal* **44**, 2217–2223.

Schraub, F.A., Kline, S.J., Henri, J., Runstadler, P.W.JR. & Little, A. 1965 Use of hydrogen bubbles for quantitative determination of time-dependent velocity fields in low-speed water flows. *J. Basic. Eng.* pp. 429–443.

Sigurdson, L. W. 1995 The structure and control of a turbulent reattaching flow. *J. Fluid Mech.* **298**, 139–165.

Sommer, F. 1965 Mehrfachlösungen bei laminaren Strömungen mit Druckinduzierter Ablösung: eine Kuspen-Katastrophe. *VDI Fortschrittsbericht, Reihe 7, Nr. 206, VDI Verlag Düsseldorf (Dissertation Bochum)* pp. 429–443.

Taneda, S. & Tomonari, Y. 1974 An experiment on the flow around a waving plate. *J. Phys. Soc. Jpn.* **36**, 1683–1689.